PROCEEDINGS OF SCIENCE

Highlights of BESIII physics

Hailong Ma (For BESIII collaboration)[a,*]

[a] *Institution of High Energy of Physics, 19B Yuquan Road, Shijingshan District, Beijing, China*

E-mail: mahl@ihep.ac.cn

Since 2009, the BESIII detector operating at the BEPCII collider has collected data samples in the center-of-mass energy region from 2.0 to 4.95 GeV. All data samples correspond to integrated luminosity of 32 fb^{-1} in total. To date, fruitful results related to τ-charm physics have been achieved from analyses of these data samples. We herein briefly introduce some highlights on the experimental studies of charmed hadrons, light hadrons, charmonium(-like) states, strangenium-like states, and baryon form factors and decay parameters.

The 10th International Workshop on Chiral Dynamics - CD2021
15-19 November 2021
Online

*Speaker

PoS(CD2021)002

1. Introduction

The Standard Model (SM) has been successful in describing almost all experimental phenomena and has been generally accepted as the fundamental theory of elementary particle physics. However, there are still many unanswered questions, which can be classified into two main categories: one for subjects related to possible new physics at unexplored energy scales and the other for non-perturbative physics, most related to Quantum Chromodynamics (QCD). Comprehensive and precise studies of e^+e^- data in the τ-charm threshold region offer ideal opportunities on the understanding of hadronization and the interplay of perturbative and non-perturbative dynamics. The BESIII detector [1] operating at the BEPCII collider is a unique and powerful facility for studying physics in the energy range from 2.0 to 4.95 GeV, with a research program that covers charmonium(-like) physics, charmed hadron physics, light hadron decays and spectroscopy, baryon form factors and τ-physics [2]. BESIII has a crucial and unique role to play in the world-wide effort to explore and characterize the behavior of QCD in the non-perturbative regime, which is one of the least understood areas of the SM.

2. Charmed hadrons

The data samples taken at $\sqrt{s}$ = 3.773, 4.178-4.226, and 4.6 GeV correspond to integrated luminosities of 2.93, 6.32, and 0.6 fb^{-1}, respectively. These are the world largest threshold charm hadron samples and provide ideal platforms to investigate the charmed hadrons $D^{0(+)}$, D_s^+, and Λ_c^+.

2.1 (Semi-)leptonic D decays

Experimental studies of (semi-)leptonic D decays are important to determine the CKM matrix elements $|V_{cs(d)}|$ describing the mixing of quark fields due to weak interaction and the decay constants of $D^+_{(s)}$ or the form factors of semileptonic D decays describing the strong interaction between initial and final state quarks. These elemental parameters are important to test CKM matrix unitarity and calibrate LQCD calculations. In addition, determinations of the ratios of the branching fractions of the (semi-)leptonic D decays into various generation leptons are important to test lepton flavor universality.

In 2014, we determined $f_{D^+}|V_{cd}| = 46.7 \pm 1.2 \pm 0.4$ MeV [3]. In 2019, we determined $f_{D^+}|V_{cd}| = 50.4 \pm 5.0 \pm 2.5$ MeV with $D^+ \to \tau^+\nu_\tau$ [4]. In 2019, we reported $f_{D_s^+}|V_{cs}| = 246.2 \pm 3.6 \pm 3.5$ MeV with muon counter method by using $D^+ \to \mu^+\nu_\mu$ based on 3.19 fb^{-1} of data taken at 4.178 GeV [5]. In 2021, we reported $f_{D_s^+}|V_{cs}| = 244.8 \pm 5.8 \pm 4.8$ MeV with $D^+ \to \tau^+\nu_\tau$ with $\tau^+ \to \rho^+\bar{\nu}\tau$ [6], $\tau^+ \to \pi^+\bar{\nu}\tau$ [7], and $\tau^+ \to e^+\bar{\nu}\tau\nu_\tau$ [8], respectively, based on 6.32 fb^{-1} of data taken between 4.178 and 4.226 GeV. With the same data sample, we also reported a slightly improved measurement of $f_{D_s^+}|V_{cs}| = 244.8 \pm 5.8 \pm 4.8$ MeV with $D^+ \to \mu^+\nu_\mu$, without using muon counter for muon identification. Figure 1 shows the fits to the $M^2_{\rm miss}$ distributions of the candidates for $D^+ \to \mu^+\nu_\mu$ and $D_s^+ \to \mu^+\nu_\mu$. Figure 2 shows comparison of $|V_{cd}|$ and $|V_{cs}|$ determined by leptonic D decays from various experiments.

By analyzing the partial decay rates of $D^0 \to K^-e^+\nu_e$ [9], $D^+ \to \bar{K}^0e^+\nu_e$ [10], $D^+ \to K_L^0e^+\nu_e$ [11], $D^0 \to K^-\mu^+\nu_\mu$ [12], $D_s^+ \to \eta e^+\nu_e$, and $D_s^+ \to \eta' e^+\nu_e$ [13], we reported the measurements of form factors of the $c \to s$ semileptonic D decays. The results are $f_+^{D\to K}|V_{cs}| = 0.717 \pm 0.003 \pm 0.004$, $f_+^{D\to K}|V_{cs}| = 0.705 \pm 0.004 \pm 0.011$, $f_+^{D\to K}|V_{cs}| = 0.720 \pm 0.006 \pm 0.011$, $f_+^{D\to K}|V_{cs}| = 0.715 \pm 0.004 \pm 0.003$, $f_+^{D_s\to \eta}|V_{cs}| = 0.446 \pm 0.005 \pm 0.004$, and $f_+^{D_s\to \eta'}|V_{cs}| = 0.477 \pm 0.049 \pm 0.011$. The latter two modes are extracted for the first time.

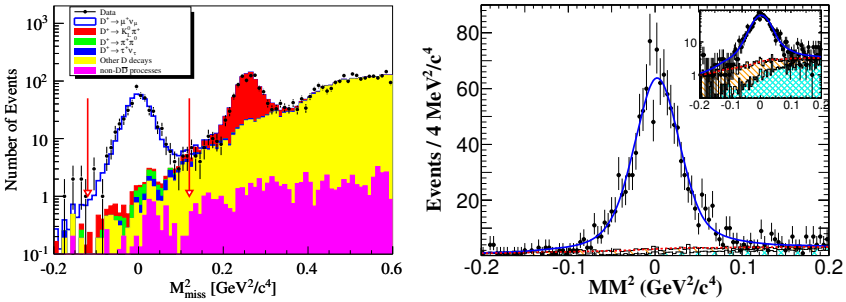

Figure 1: The $M^2_{\rm miss}$ distributions of the candidates for $D^+ \to \mu^+\nu_\mu$ (left) and $D_s^+ \to \mu^+\nu_\mu$ (right).

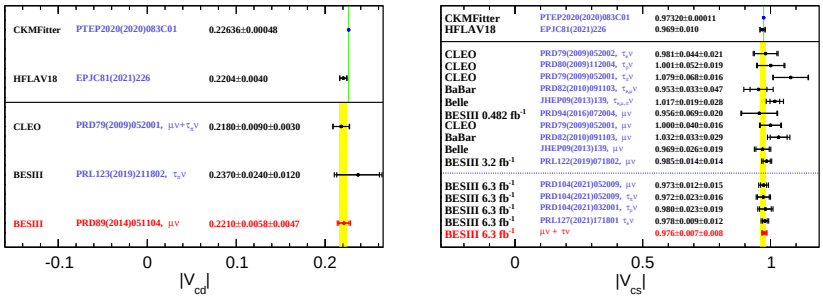

Figure 2: Comparison of $|V_{cd}|$ and $|V_{cs}|$ measured with leptonic D decays from various experiments. Green bands are $\pm1\sigma$ borders of the standard model global fit while yellow bands are $\pm1\sigma$ borders of the averages.

By analyzing the partial decay rates of $D^0 \to \pi^- e^+ \nu_e$ [9], $D^+ \to \pi^0 e^+ \nu_e$ [10], $D^+ \to \eta e^+ \nu_e$ [14], $D^+ \to \eta e^+ \nu_e$ [15], and $D_s^+ \to K^0 e^+ \nu_e$ [16], we reported the measurements of form factors of the $c \to d$ semileptonic D decays. The results are $f_+^{D\to\pi}|V_{cd}| = 0.144 \pm 0.002 \pm 0.001$, $f_+^{D\to\pi}|V_{cd}| = 0.140 \pm 0.003 \pm 0.001$, $f_+^{D\to\eta}|V_{cd}| = 0.079 \pm 0.006 \pm 0.002$, $f_+^{D\to\eta}|V_{cd}| = 0.087 \pm 0.008 \pm 0.002$, and $f_+^{D_s\to K}|V_{cd}| = 0.162 \pm 0.019 \pm 0.003$. The latter two modes are extracted for the first time.

We reported the improved measurements of the branching fractions of $D^0 \to K^-\mu^+\nu_\mu$, $D^0 \to \pi^-\mu^+\nu_\mu$, $D^+ \to \bar{K}^0\mu^+\nu_\mu$, $\Lambda_c^+ \to \Lambda\mu^+\nu_\mu$, and $D_s^+ \to \ell^+\nu_\ell$, and the first measurements of the branching fractions of $D^0 \to \rho^-\mu^+\nu_\mu$, $D^+ \to \pi^0\mu^+\nu_\mu$, $D^+ \to \eta\mu^+\nu_\mu$, $D^+ \to \omega\mu^+\nu_\mu$, $D_s^+ \to \phi\mu^+\nu_\mu$, $D_s^+ \to \eta\mu^+\nu_\mu$, $D_s^+ \to \eta'\mu^+\nu_\mu$, and $D_s^+ \to \tau^+\nu_\tau$. Combining with previous measurements or world average values of their individual semielectronic or tauonic counterparts gave tests of lepton flavor universality with various processes. The reported branching fraction ratios are $\mathcal{B}(D^0 \to K^-\mu^+\nu_\mu)/\mathcal{B}(D^0 \to K^-e^+\nu_e) = 0.978 \pm 0.007 \pm 0.012$ [12], $\mathcal{B}(D^0 \to \pi^-\mu^+\nu_\mu)/\mathcal{B}(D^0 \to \pi^-e^+\nu_e) = 0.922 \pm 0.030 \pm 0.022$ [17], $\mathcal{B}(D^0 \to \rho^-\mu^+\nu_\mu)/\mathcal{B}(D^0 \to \rho^-e^+\nu_e) = 0.90 \pm 0.111$ [18], $\mathcal{B}(D^+ \to \bar{K}^0\mu^+\nu_\mu)/\mathcal{B}(D^+ \to \bar{K}^0e^+\nu_e) = 1.00 \pm 0.03$ [19], $\mathcal{B}(D^+ \to \pi^0\mu^+\nu_\mu)/\mathcal{B}(D^+ \to \pi^0e^+\nu_e) = 0.964 \pm 0.037 \pm 0.026$ [17], $\mathcal{B}(D^+ \to \eta\mu^+\nu_\mu)/\mathcal{B}(D^+ \to \eta e^+\nu_e) = 1.05 \pm 0.14$ [15], $\mathcal{B}(D^+ \to \omega\mu^+\nu_\mu)/\mathcal{B}(D^+ \to \omega e^+\nu_e) = 0.91 \pm 0.13$ [20], $\mathcal{B}(D_s^+ \to \phi\mu^+\nu_\mu)/\mathcal{B}(D_s^+ \to \phi e^+\nu_e) = 1.05 \pm 0.24$ [21], $\mathcal{B}(D_s^+ \to \eta\mu^+\nu_\mu)/\mathcal{B}(D_s^+ \to \eta e^+\nu_e = 0.86 \pm 0.29$ [21], $\mathcal{B}(D_s^+ \to \eta'\mu^+\nu_\mu)/\mathcal{B}(D_s^+ \to \eta' e^+\nu_e) = 1.14 \pm 0.68$ [21], $\mathcal{B}(\Lambda_c^+ \to \Lambda\mu^+\nu_\mu)/\mathcal{B}(\Lambda_c^+ \to \Lambda e^+\nu_e) = 0.96 \pm 0.16 \pm 0.04$ [22]. $\mathcal{B}(D^+ \to \tau^+\nu_\tau)/\mathcal{B}(D^+ \to \tau^+\nu_\tau) = 3.21 \pm 0.64 \pm 0.43$ [4], and $\mathcal{B}(D_s^+ \to \tau^+\nu_\tau)/\mathcal{B}(D_s^+ \to \tau^+\nu_\tau) = 9.67 \pm 0.36$ [8]. These ratios are all consistent with individual SM predicted values within 2σ. The ratios of partial decay rates in various q^2 intervals for $D^0 \to K^-\ell^+\nu_\ell$, $D^0 \to \pi^-\ell^+\nu_\ell$, and $D^+ \to \pi^0\ell^+\nu_\ell$ have also been examined, and no more than

2σ deviation has been found.

Figure 3 shows the fit to the partial decay rates, projection to $f_+^K(q^2)$ for $D^0 \to K^-\mu^+\nu_\mu$ and the measured branching fraction ratio $\mathcal{R}_{\mu/e}$ in each q^2 interval.

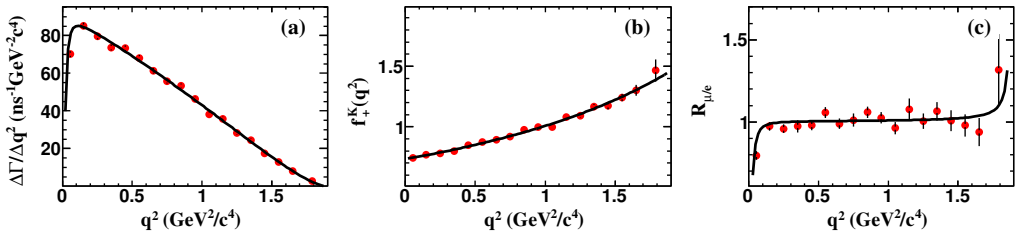

Figure 3: (a) Fit to the partial decay rates, (b) projection to $f_+^K(q^2)$ for $D^0 \to K^-\mu^+\nu_\mu$ and (c) the measured branching fraction ratio $\mathcal{R}_{\mu/e}$ in each q^2 interval.

Semileptonic D decays into light mesons provide clean environment to investigate the property of light mesons. In 2018, we reported the first observation of $D^{0(+)} \to a_0(980)^{-(0)}e^+\nu_e$ via $a_0(980)^{-(0)} \to \pi^{-(0)}\eta$ [23]. In 2019, we reported the first observation of $D^+ \to f_0(500)e^+\nu_e$ and search for $D^+ \to f_0(980)e^+\nu_e$ from a combined analysis of $D^{0(+)} \to \pi^{0(+)}\pi^-e^+\nu_e$ [24]. The reported branching fractions give $(\mathcal{B}(D^+ \to f_0(500)e^+\nu_e) + \mathcal{B}(D^+ \to f_0(980)e^+\nu_e))/\mathcal{B}(D^+ \to a_0(980)^0e^+\nu_e > 2.7$ [24]. This ratio supports the theoretical prediction under the hyperthesis that a_0 and f_0 consist of tetraquark. Also, we reported the first observations of $D^+ \to \bar{K}_1(1270)^0e^+\nu_e$ [25] and $D^0 \to K_1(1270)^-e^+\nu_e$ [26] via $\bar{K}_1(1270) \to K^-\pi^+\pi^{0(-)}$. The reported branching fractions are important to understand the K_1 mixing angle and open an ideal window to explore the property and nature of axial-vector mesons of K_1.

2.2 Strong phase difference of neutral D decays

In B physics, precision measurements of CP violation phase angles α, β, and γ offer powerful tests on the electro-weak theories. Among them, the γ precision is the most urgent to improve. However, precision measurements of γ at LHCb and Belle II need input strong phase difference of neutral D decays. Quantum-correlated $e^+e^- \to \psi(3770) \to D^0\bar{D}^0$ pairs at BESIII offer an ideal opportunity to extract the strong phase difference between D^0 and $\bar{D}^0$. In the future 10-15 years, the statistical uncertainties of measuring γ at LHCb upgrade and Belle II are hopefully to reach at 0.4° and 1.5°, respectively. Nevertheless, the constraint on the γ measurement using the previous CLEO data is only 2°. Improved measurements of the strong phase difference between D^0 and $\bar{D}^0$ are highly desirable.

BESIII reported measurements of the strong phase differences between D^0 and $\bar{D}^0$ of $K^0_{S/L}\pi^+\pi^-$ [27], $K^0_{S/L}K^+K^-$ [28], $K^\pm\pi^\mp\pi^\mp\pi^\pm$ and $K^\pm\pi^\mp\pi^0$ [29]. With these parameters as inputs, the constraints on the future γ measurements with the corresponding D decay modes are hopefully to be reduced to $< 0.9^\circ$, 1.3°, and 6°, respectively. Figure 4 shows the obtained strong phase difference (c_i, s_i) between D^0 and $\bar{D}^0$ decays into $K^0_{S/L}\pi^+\pi^-$ in various binning schemes.

2.3 Absolute branching fractions of Λ_c^+ decays

The Λ_c^+ is the lightest one in the family of charmed baryons. Although it was first observed in 1970s, there was no direct measurement of the branching fractions of Λ_c^+ decays before BESIII. Previously, the experimental studies of Λ_c^+ decays were usually made relative to the reference mode of $\Lambda_c^+ \to pK^-\pi^+$ with high background and large uncertainties ($> 25\%$), and about half of Λ_c^+ decays remained unknown.

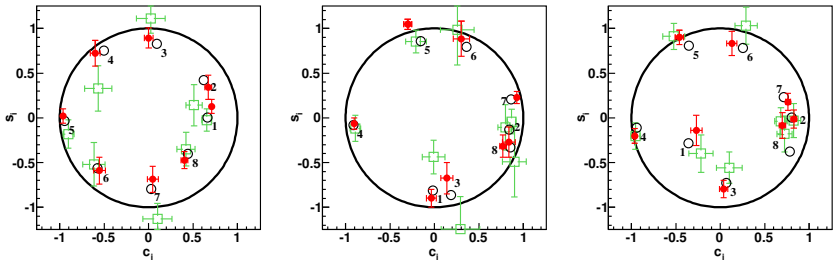

Figure 4: Strong phase difference (c_i, s_i) between D^0 and $\bar{D}^0$ decays into $K^0_{S/L}\pi^+\pi^-$.

We reported the direct measurements of the branching fractions of $\Lambda_c^+ \to \Lambda e^+\nu_e$ [30] and $\Lambda_c^+ \to pK^-\pi^+$ [31], the first observation of $\Lambda_c^+ \to nK_S^0\pi^+$ [32], the improved measurements of $\Lambda_c^+ \to pK^+K^-$ and $p\pi^+\pi^-$ [33], the inclusive decays of $\Lambda_c^+ \to \Lambda X$ [34] and $\Lambda_c^+ \to e^+\nu_e X$ [35] as well as some other decays. As an example, Fig. 5 shows the fits to the $M_{\rm BC}$ distributions of various hadronic Λ_c^+ decays and the $U_{\rm miss}$ distribution of $\Lambda_c^+ \to \Lambda e^+\nu_e$. The precisions of the obtained branching fractions for known decay modes are improved significantly and some new decay modes are observed for the first time. These results have a great significance on the charmed baryon field.

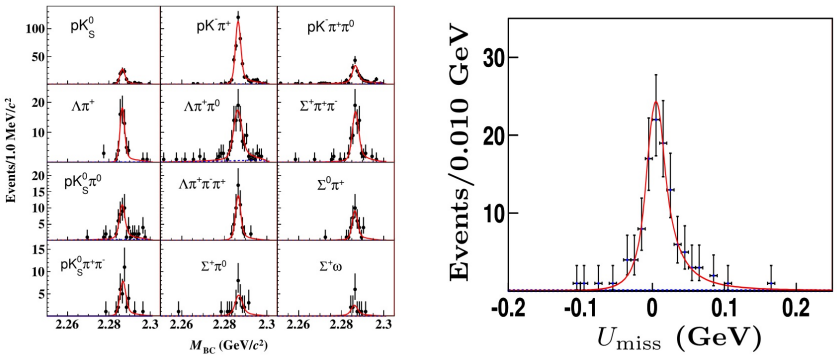

Figure 5: Fits to the $M_{\rm BC}$ distributions of various hadronic Λ_c^+ decays (left) and the $U_{\rm miss}$ distribution of $\Lambda_c^+ \to \Lambda e^+\nu_e$ (right).

3. Light hadrons

The generally accepted theory for the strong interaction, QCD, remains a challenging part of the standard model in the low- and mediumenergy regime. In the high energy regime, asymptotic freedom of the partons constituting hadrons allows systematic calculations in QCD using perturbation theory. In the low-energy regime where the energies are (much) smaller than a typical strong interaction scale, there are well-established theoretical methods, chiral perturbation theory (ChPT). In the intermediate-energy regime, the non-Abelian character of QCD requires a non-perturbative approach which must rely either on lattice QCD or on QCDinspired models. Therefore, the study of light hadrons is central to the understanding of confinement physics.

3.1 $X(1835)$, $X(2120)$, and $X(2370)$ states

Anomalous strong $p\bar{p}$ threshold enhancement structure was first observed by BESII in $J/\psi \to \gamma p\bar{p}$ [36]. It was confirmed by BESIII with much higher significance [37]. The mass and width are determined to be $1836.5^{+19+18}_{-5\ -17} \pm 19$ MeV/c^2 and < 76 MeV (90% C.L.). The spin-parity of this structure is determined to be $J^{PC} = 0^{-+}$. The $X(1835)$ was first observed by BESII in $J/\psi \to \gamma\eta'\pi^+\pi^-$ [38]. It was confirmed by BESIII with much higher significance in [39]. The reported mass and width are $1836.5 \pm 3.0^{+5.6}_{-2.1}$ MeV/c^2 and $190 \pm 9^{+38}_{-36}$ MeV, respectively. Figure 6 shows the structures around $p\bar{p}$ production threshold in $M_{p\bar{p}}$ and $M_{\pi^+\pi^-\eta}$ spectra at BESIII. These two structures have close masses but very different widths.

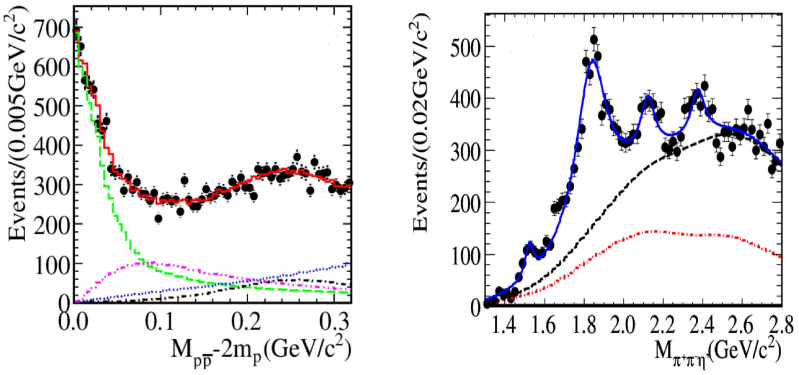

Figure 6: Structures around $p\bar{p}$ production threshold in $M_{p\bar{p}}$ (left) and $M_{\pi^+\pi^-\eta}$ (right) spectra.

Afterwards, we reported a few structures around 1835 MeV/c^2 in the invariant mass spectra of $\eta\pi^+\pi^-$, $\phi\omega$, $3(\pi^+\pi^-)$, $K^0_S K^0_S\eta$, $\eta'\pi^+\pi^-$, and $\gamma\phi$ in $J/\psi \to \omega\eta\pi^+\pi^-$ [40], $\gamma\phi\omega$ [41], $\gamma 3(\pi^+\pi^-)$ [42], $K^0_S K^0_S\eta$ [43], $\gamma\eta'\pi^+\pi^-$ [44], $\gamma\gamma\phi$ [45]. Figure 7 shows the measured masses versus widths of the structures around 1835 MeV/c^2 from different processes at BESIII. Further studies of the fine line-shapes of $X(1835)$ in more decay modes will provide conclusive information on the nature of these states.

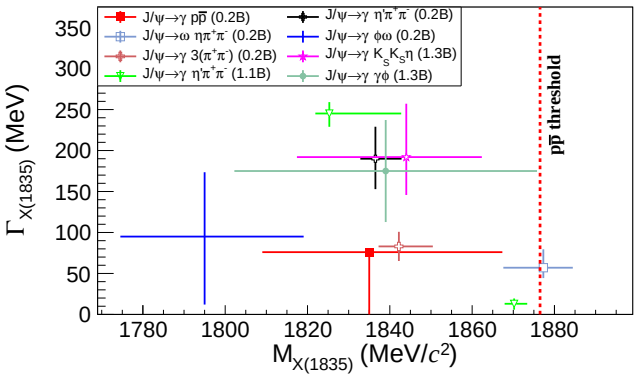

Figure 7: Masses versus widths of the structures around 1835 MeV obtained from different processes.

Meanwhile, we also observed the $X(2120)$ and $X(2370)$, which may be potential candidates of glueball states, in $J/\psi \to \gamma\eta'\pi^+\pi^-$ [39, 44]. In 2020, we reported the first observation of $X(2370) \to K\bar{K}\eta'$ in $J/\psi \to \gamma K\bar{K}\eta'$ but did not find evidence for $X(2120) \to K\bar{K}\eta'$. The mass and width of $X(2370)$ are $2341.6 \pm 6.5 \pm 5.7$ MeV/c^2 and $117 \pm 10 \pm 8$ MeV [46]. In 2021, we reported search for $X(2370) \to \eta\eta\eta'$ in $J/\psi \to \gamma\eta\eta\eta'$ and no evidence was found [47].

3.2 Absolute branching fractions of light hadron or baryon decays

The world largest J/ψ sample also offers an ideal platform to determine the absolute branching fractions of light mesons or baryons. For example, via the $J/\psi \to \gamma\eta'$ channel, the branching fractions of $\eta' \to \gamma\pi^+\pi^-$, $\eta\pi^+\pi^-$, $\eta\pi^0\pi^0$, $\gamma\omega$ and $\gamma\gamma$ are determined to be $(29.90 \pm 0.03 \pm 0.55)\%$, $(41.24 \pm 0.08 \pm 1.24)\%$, $(21.36 \pm 0.10 \pm 0.92)\%$, $(2.489 \pm 0.018 \pm 0.074)\%$, and $(2.331 \pm 0.012 \pm 0.035)\%$ [48], respectively. Compared to individual world averages, the former three have comparable precision while the latter two have much improved precision. Via the $J/\psi \to \Lambda\bar{\Lambda}$ channel, the branching fraction of $\Lambda \to p\mu^-\nu_\mu$ is determined to be $(1.48 \pm 0.21 \pm 0.08) \times 10^{-4}$ [49]. Combining with the world average of the branching fraction of $\Lambda \to pe^-\nu_e$ gives the branching fraction ratio of $\mathcal{B}(\Lambda \to p\mu^-\nu_\mu)/\mathcal{B}(\Lambda \to pe^-\nu_e) = 0.178 \pm 0.028$, which is consistent with theoretical calculation, thereby indicating no violation of lepton flavor universality.

4. Charmonium(-like) states

Before the discovery of the $X(3872)$ at Belle in 2003, every meson in the mass region between 2.9 and 4.5 GeV/c^2 could be successfully described as a $c\bar{c}$ bound state. Simple potential models, using QCD-inspired potentials binding quarks and antiquarks, could reproduce the spectrum of charmonium states all the way from the $\eta_c(1S)$ (the ground state) up to the $\psi(4415)$ (usually considered to be the third radial excitation of the J/ψ). This simple model of the charmonium spectrum has since broken down in a dramatic fashion.

4.1 X states

The $X(3872)$ was first observed in $B^\pm \to K^\pm\pi^+\pi^- J/\psi$ decay by Belle [50]. It was later studied in B decays, $p\bar{p}$, pp, or e^+e^- collision by Belle, BaBar, D0, CDF2, LHCb, and BESIII. The discovery of the $X(3872)$ quickly led to the discovery of many more states with exotic configurations of quarks and gluons. In 2014, BESIII reported the first study of $X(3872)$ via $e^+e^- \to Y(4260) \to \gamma X(3872) \to \gamma\pi^+\pi^- J/\psi$ process with 3 fb^{-1} of data at $\sqrt{s}$ =4.009 to 4.42 GeV [51]. In recent years, with larger data samples, BESIII reported more studies of $X(3872)$ states via $e^+e^- \to \gamma X(3872) \to \gamma\pi^0\chi_{c1}$ [52], $\gamma\pi^+\pi^- J/\psi$ and $\gamma\omega J/\psi$ [53] as well as $\gamma D^0\bar{D}^{*0}$ [54]. In [54], an evidence of $X(3872) \to \gamma J/\psi$ was found but no evidence of $X(3872) \to \gamma\psi(3686)$ was found. Figure 8 shows the $X(3872)$ signals in various processes and the line-shapes of cross sections for $e^+e^- \to \gamma\pi^+\pi^- J/\psi$ and $\gamma\omega J/\psi$ at BESIII.

4.2 Y states

The Y is charmonium-like state with $J^{PC} = 1^{--}$, which can be studied in ISR or direct e^+e^- annihilation. Following the discovery of the $X(3872)$, the $Y(4260)$ was first observed in $e^+e^-(\gamma_{\rm ISR}) \to \pi^+\pi^- J/\psi$ process by BaBar [55]. The $Y(4260)$ and $Y(4660)$ were observed in $e^+e^-(\gamma_{\rm ISR}) \to \pi^+\pi^-\psi(3686)$ process by BaBar [56]. In recent years, BESIII reported more studies of Y states by analyzing the line-shapes of cross sections for $e^+e^- \to \pi^+\pi^- J/\psi$ [57], $\pi^+\pi^- h_c$ [58], $\pi^+ D^0 D^{*-} + c.c.$ [59], $\omega\chi_{c0}$ [60], $\eta J/\psi$ [61], $\pi^0\pi^0 J/\psi$ [62], $\pi^+\pi^-\psi(3686)$ [63], $\mu^+\mu^-$ [64], $\eta' J/\psi$ [65], and $\eta_c\pi^+\pi^-\pi^0$ [66]. The $Y(4220)$ was found in all these processes, while the $Y(4360)$ and $Y(4660)$ were found only in some of them. Figure 10 shows the masses versus widths of the $Y(4220)$ and $Y(4360)$ obtained from different processes. More experimental and theoretical studies are expected to deeply understand the nature and properties of these states as well as their possible connections.

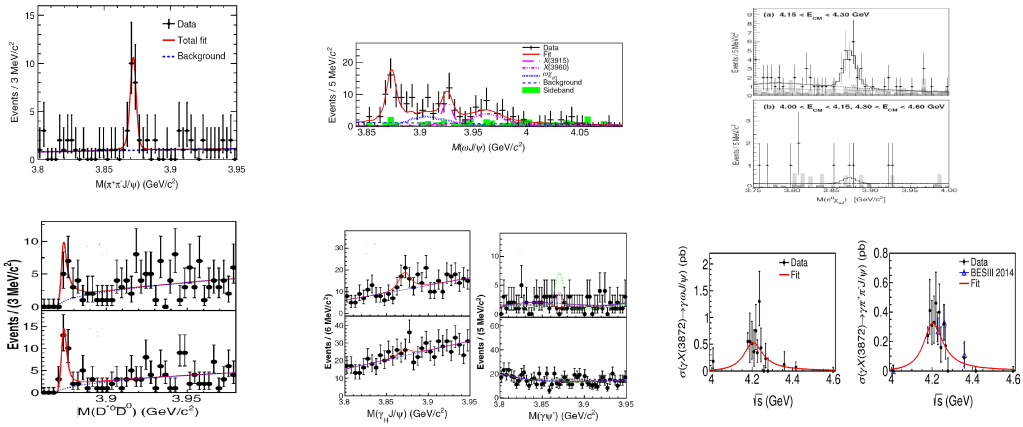

Figure 8: The $X(3872)$ signals in various processes (top left, top middle, top right, bottom left, bottom middle) and the line-shapes of cross sections for $e^+e^- \to \gamma\omega J/\psi$ and $\gamma\pi^+\pi^- J/\psi$ (bottom right) at BESIII.

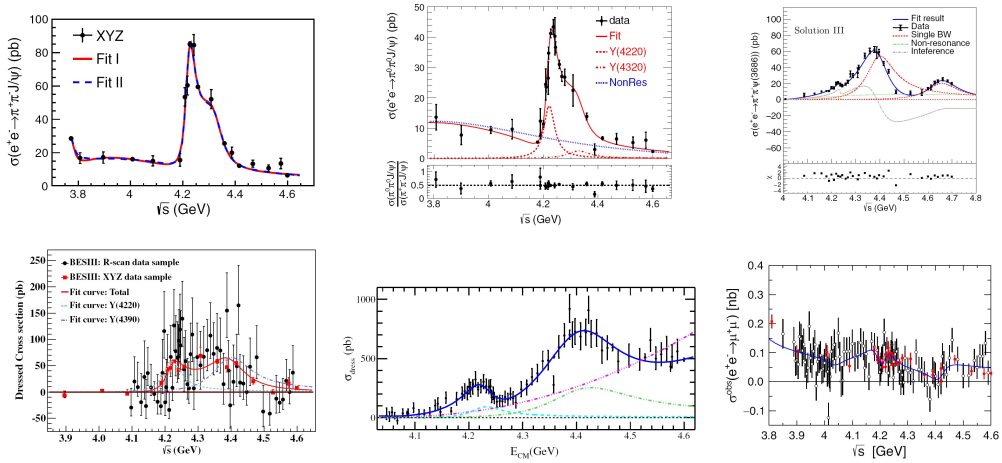

Figure 9: The Y states in the processes of $e^+e^- \to \pi^+\pi^- J/\psi$ (top left), $\pi^0\pi^0 J/\psi$ (top middle), $\pi^+\pi^-\psi(3686)$ (top right), $\pi^+\pi^- h_c$ (bottom left), $\pi^+ D^0 D^{*-} + c.c.$ (bottom middle), and $\mu^+\mu^-$ (bottom right) at BESIII.

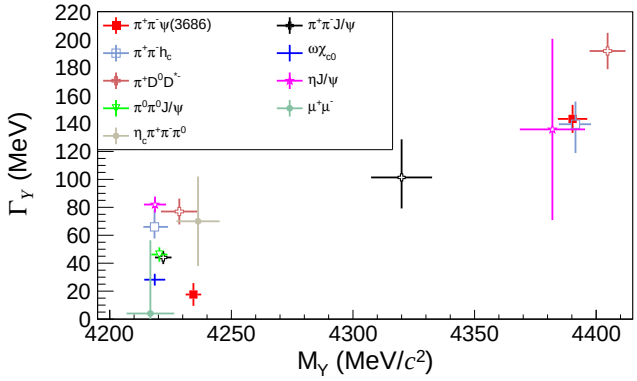

Figure 10: Masses versus widths of the $Y(4220)$ and $Y(4360)$ obtained from different processes at BESIII.

4.3 Z states

By examining the mass spectra of $\pi^{\pm}J/\psi$, $\pi^0 J/\psi$, $\pi^{\pm}h_c$, $\pi^0 h_c$, $(D\bar{D}^*)^{\pm}$, $(D\bar{D}^*)^0$, $(D^*\bar{D}^*)^{\pm}$, $(D^*\bar{D}^*)^0$ from analyses of the processes of $e^+e^- \to \pi^+\pi^- J/\psi$, $\pi^0\pi^0 J/\psi$, $\pi^+\pi^- h_c$, $\pi^0\pi^0 h_c$, $\pi^{\mp}(D\bar{D}^*)^{\pm}$, $\pi^0(D\bar{D}^*)^0 + c.c.$, $\pi^{\mp}(D^*\bar{D}^*)^{\pm}$, and $\pi^0(D^*\bar{D}^*)^0 + c.c.$, we reported the first observations of charmonium-like states: $Z_c(3900)^{\pm}$, $Z_c(3900)^0$, $Z_c(3885)^{\pm}$, $Z_c(3885)^0$, $Z_c(4020)^{\pm}$, $Z_c(4020)^0$, $Z_c(4025)^{\pm}$, and $Z_c(4025)^0$. As example, the former four subplots of Fig. 11 show individual invariant mass spectra of the candidates for $Z_c(3900)^{\pm}$, $Z_c(3885)^{\pm}$, $Z_c(4020)^{\pm}$, and $Z_c(4025)^{\pm}$. Table 1 summarizes the reported masses and widths of these states. These Z_c states are observed in both charged and neutral modes.

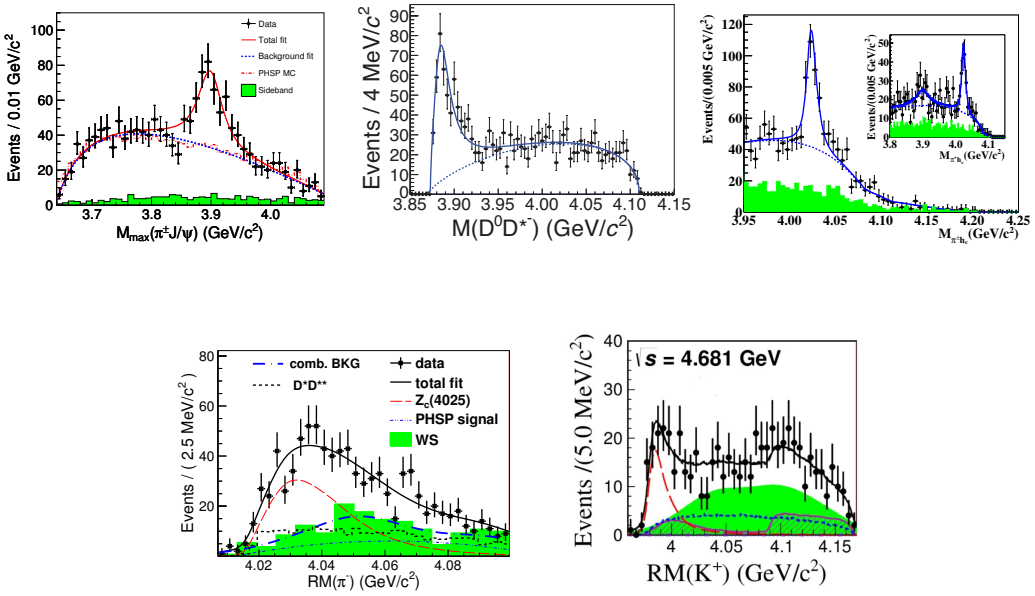

Figure 11: The signals of $Z_c(3900)^{\pm}$ (top left), $Z_c(3885)^{\pm}$ (top middle), $Z_c(4020)^{\pm}$ (top right), $Z_c(4025)^{\pm}$ (bottom left) and $Z_{cs}(4680)$ (bottom right) observed at BESIII.

Table 1: The masses, widths, and decay modes, and references for various Z_c states.

State	Mass (MeV/c^2)	Width (MeV)	Decay mode	Reference
$Z_c(3900)^{\pm}$	$3899.0 \pm 3.6 \pm 3.7$	$46 \pm 10 \pm 20$	$\pi^{\pm}J/\psi$	[67]
$Z_c(3900)^0$	$3894.8 \pm 2.3 \pm 2.7$	$29.6 \pm 8.2 \pm 8.2$	$\pi^0 J/\psi$	[68]
$Z_c(3885)^{\pm}$	$3883.9 \pm 1.5 \pm 4.2$	$24.8 \pm 3.3 \pm 11.0$	$(D\bar{D}^*)^{\pm}$	[69]
$Z_c(3885)^0$	$3881.7 \pm 1.6 \pm 2.1$	$26.6 \pm 2.0 \pm 2.3$	$(D\bar{D}^*)^0$	[70]
$Z_c(3885)^{\pm}$	$3885.7^{+4.3}_{-5.7} \pm 8.4$	$35^{+11}_{-12} \pm 15$	$(D\bar{D}^*)^{\pm}$	[71]
$Z_c(4020)^{\pm}$	$4022.9 \pm 0.8 \pm 2.7$	$7.9 \pm 2.7 \pm 2.7$	$\pi^{\pm}h_c$	[72]
$Z_c(4020)^0$	$4023.9 \pm 2.2 \pm 3.8$	Fixed	$\pi^0 h_c$	[73]
$Z_c(4025)^{\pm}$	$4026.3 \pm 2.6 \pm 3.7$	$24.8 \pm 5.6 \pm 7.7$	$(D^*\bar{D}^*)^{\pm}$	[74]
$Z_c(4025)^0$	$4025.5^{+2.0}_{-4.7} \pm 3.1$	$23.0 \pm 6.0 \pm 1.0$	$(D^*\bar{D}^*)^0$	[75]

Given tentraquark state assumption, it is naviely expected that there exists SU(3) parter Z_{cs} with strangeness quark. In 2021, BESIII reported the first observation of $Z_{cs}(4680)$ in the open charm process of $e^+e^- \to K^+(D_s^- D^{*0} + D_s^{*-} D^0) + c.c.$, as shown in Fig. 11(bottom right), by using the data sample taken around 4.68 GeV [76]. Its mass and width are determined to be $3985.2^{+2.1}_{-2.0} \pm 1.7$

MeV/c^2 and $13.8^{+8.1}_{-5.2} \pm 4.9$ MeV, respectively. Later, LHCb reported an observation of $Z_{cs}(4000)^+$ in the hidden charm process of $B^+ \to \phi J/\psi K^+$ with mass of $4003 \pm 6^{+4}_{-14}$ MeV/c^2 and width of $131 \pm 15 \pm 26$ MeV [77]. These two states have close masses but very different widths.

In the past decade, a series of charmonium(-like) states, e.g., X, Y, and Z states, were observed at BESIII. These new configurations, as potential candidates for tetraquarks, hadronic molecules, and hybrid mesons, allow us to probe the mysterious non-perturbative QCD which underlies the way quarks and gluons combining into larger hadronic composites.

4.4 Charmless decays of ψ states above open charm threshold

In 2008, BESII reported an anomalous line-shape of cross section for $e^+e^- \to$ inclusive hadrons in the energy region from 3.65 to 3.89 GeV. This line-shape can be well described when fitted by a dis-structure, e.g., a structure around traditional $\psi(3770)$ plus an additional structure $R(3760)$ [78], with significance of 7σ. In 2021, BESIII reported a measurement of line-shape of cross section for $e^+e^- \to J/\psi X$ in a similar energy region [79]. Compared to a single $\psi(3770)$ resonance assumption, the significance of the fit to this line-shape under the aforementioned di-structure assumption is 5.3σ. The fit result is shown in Fig. 12(left).

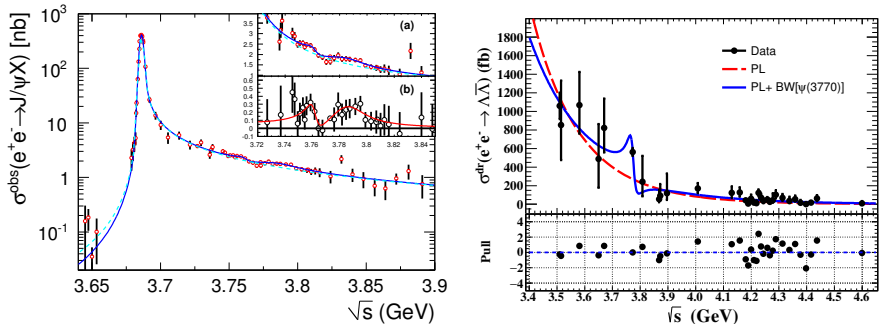

Figure 12: Fits to the line-shapes of cross sections of $e^+e^- \to J/\psi X$ (left) and $e^+e^- \to \Lambda\bar{\Lambda}$ (right).

Based on the BESII and CLEO measurements, the particle data group gives the branching fraction of $\psi(3770) \to \text{non}-D\bar{D}$ to be $(93^{+8}_{-9})\%$. This leaves large room for possible charmless decays of $\psi(3770)$. Except for $\psi(3770) \to \phi\eta$, however, no other charmless decays for charomonium states above open charm threshold have been reported. BESIII reported an analysis of the line-shape of cross section for $e^+e^- \to \Lambda\bar{\Lambda}$ in the energy range between 3.5 and 4.6 GeV [80], as shown in Fig. 12(right). A signal of $\psi(3770) \to \Lambda\bar{\Lambda}$ is found with significance of 4.9σ. Its decay branching fraction is determined to be $(2.4^{+15.0}_{-1.9}) \times 10^{-5}$ and $(14.4^{+2.7}_{-14.0}) \times 10^{-5}$ for two different interference angles between the resonance and continuum amplitudes. Meanwhile, the energy dependence of cross section of continuum light hadron, $1/E^n_{\rm cm}$, is obtained to be $n = 8.2 \pm 0.6$, which significantly deviates from simple $1/E^2_{\rm cm}$ relation in the searches for $\psi(3770) \to$ light hadron decays in previous BESII and CLEO works.

Also, we reported the line-shapes of cross sections for $e^+e^- \to K^+K^-\pi^+\pi^-$, $2(K^+K^-)$, $K^+K^-\pi^+\pi^-\pi^0$, $2(K^+K^-)\pi^0$, $2(\pi^+\pi^-)$, $p\bar{p}\pi^+\pi^-$, $2(\pi^+\pi^-)\pi^0$, $p\bar{p}\pi^+\pi^-\pi^0$ in the energy region between 3.8 and 4.6 GeV [81]. The fits to these line-shapes indicate that the cross section energy dependencies for all processes significantly deviate from simple $1/E^2_{\rm cm}$ relation. In addition, an evidence of $\psi(4040) \to 2(\pi^+\pi^-)\pi^0$ is reported with significance of 3.6σ. Its decay branching fraction is determined to be $(3.51 \pm 1.89 \pm 1.24) \times 10^{-5}$ and $(2.41 \pm 0.05 \pm 0.79) \times 10^{-5}$ for two different interference angles between the resonance and continuum amplitudes.

5. Strangenium-like states

Quarkonia provide a unique platform to study QCD. Substantial progress has been made over the recent years from the investigation of charmonia ($c\bar{c}$) and bottomonia ($b\bar{b}$). A plethora of interesting new hadronic states were found. New types of hadronic matter, such as hybrids, multiquark states, and hadronic molecules with (hidden) charm and bottom quarks are considered in the interpretation. The multitude of results from heavier quarkonia leads to the obvious question whether similar states should exists in the strange sector. However, experimental evidence for a rich spectrum of strangeonium ($s\bar{s}$) or new types of hadronic matter with strange quarks is scarce.

The strangenium-like state, $\phi(2170)$, previously referred to as $Y(2175)$, was first observed in $e^+e^-(\gamma_{\rm ISR}) \to \phi f_0(980)$ process by BaBar [82]. Subsequent studies in $e^+e^-(\gamma_{\rm ISR}) \to \phi f_0(980)$ process by Belle [83] and $J/\psi \to \eta\phi f_0(980)$ process by BESII [84]. In recent years, BESIII reported some structures around $\phi(2170)$ in the processes of $e^+e^- \to \phi K^+K^-$ [85], K^+K^- [86], and $K^+K^-\pi^0\pi^0$ [87], $\phi\eta'$ [88] (shown in Fig. 13(left) for example), $\phi\eta$ [89], $K^0_SK^0_L$ [90], and $\omega\eta$ [91], as well as in the decay of $J/\psi \to \eta\phi\eta'$ [92]. Figure 13(right) shows the comparison of the determined masses and widths from the fits to the line-shapes of the cross sections of various processes. They are very different with each other. To date, limited decay modes of $\phi(2170)$ have been found and its nature is still mysterious. More studies in both experiments and theories are highly desirable.

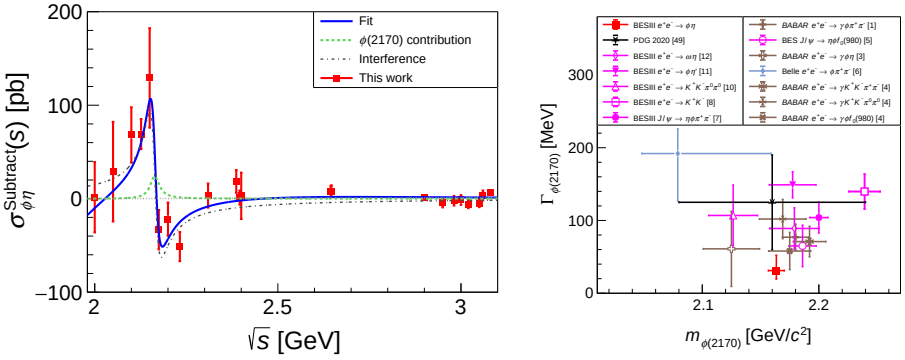

Figure 13: Fit to the born cross section of $e^+e^- \to \phi\eta$ (left) and the comparison of the masses and widths of structures around $\phi(2170)$ from different processes at various experiments.

6. Baryon form factors and decay parameters

Baryons provide a unique window to the strong interaction, since they constitute the simplest system for which the non-Abelian nature of QCD is manifest. The inner structure of baryons can be described and studied experimentally on a common footing through electromagnetic form factors, probed by processes involving hadrons interacting with virtual photons. The electromagnetic form factors are fundamental observables of non-perturbative QCD and quantify the deviation from the point-like case. The form factors of baryons in space-like region and time-like region are usually described by real and complex forms, respectively. In the time-like region, the electro-magnetic form factors of baryons characterize the internal structure of the baryons, which can be measured via e^+e^- annihilation or charmonium decays at BESIII.

The electric and magnetic form factors are usually denoted as $G_E(q^2)$ and $G_M(q^2)$, respectively. BESIII reported the measurements of the proton form factors [93–96] by using e^+e^- collision

data or ISR method with various data samples from 2.232 to 3.671, 2.00 to 3.08, 3.773 to 4.6 and 3.773 to 4.6 GeV, respectively. Average cross section near threshold is about 840 pb and is close to cross section at threshold under point-like hypothesis. The $G_E(q^2)$ and $G_M(q^2)$ are determined with high accuracy comparable to the space-like data.

In [97], we reported the measurement of the born cross section for $e^+e^- \to n\bar{n}$ in energy region from 2.0 to 3.08 GeV with much improved precision and in larger energy region than before. The results agree with the theoretical prediction and thereby clarify the "long-standing puzzle" that the γn coupling is larger than the γp coupling. BESIII's measurement [96] comfirmed the periodic behavior of the proton form factors, with result shown in Fig. 14(left), which was first observed at BaBar. Similar periodic behavior of the neutron form factors was observed at BESIII [97], with result shown in Fig. 14(right), for the first time. Simultaneously fitting to the p and n data gives the shared frequency (5.55 ± 0.28) GeV^{-1} and with phase difference $(125 \pm 12)^\circ$.

By analyzing the $e^+e^- \to \Lambda\bar{\Lambda}$ signals from data at 2.396 GeV, we confirmed the complex form of electromagnetic form factors [98]. The ratio of between electronic and magnetic form factors is determined to be $\frac{G_E}{G_M} = 0.96 \pm 0.14 \pm 0.02$ with phase difference of $(37 \pm 12 \pm 6)^\circ$.

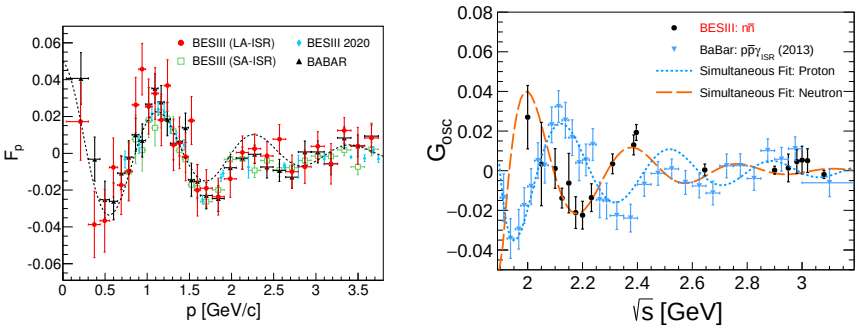

Figure 14: Periodic behaviors observed in the proton (left) and neutron (right) form factors.

Moreover, we reported a very precise measurement of the Λ decay asymmetry by using $J/\psi \to \Lambda\bar{\Lambda}$ events [99]. Figure 15(left) shows the obtained transverse polarization dependence on $\cos\theta_\Lambda$. The phase difference between Λ and $\bar{\Lambda}$ is determined to be $(42.4 \pm 0.6 \pm 0.5)^\circ$. Our result corrects a long-historical underestimation of Λ decay asymmetry. In addition, similar behavior of the transverse polarization dependence of Σ^+, as shown in Fig.15(right), was also found in an analysis of $J/\psi \to \Sigma^+\bar{\Sigma}^-$ and $\psi(3686) \to \Sigma^+\bar{\Sigma}^-$ events [100].

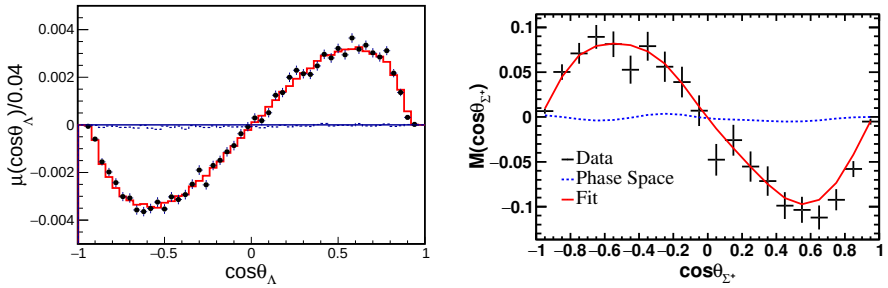

Figure 15: Transverse polarization dependence on $\cos\theta_\Lambda$ (left) and $\cos\theta_\Sigma$ (right) in individual decays.

7. Summary

BESIII is the only hadron-physics experiment in the world that exploits electron-positron annihilation in the τ-charm energy region. Since 2009, the BESIII experiment has been running successfully and has collected about $32\,\mathrm{fb}^{-1}$ of integrated luminosity data in the center-of-mass energy region from 2.0 to 4.95 GeV. To date, the physics output comprises more than 360 papers in highly-ranked peer-reviewed journals, covering the physics related to charmed hadrons, light hadrons, charmonium(-like) states, strangenium-like states, R values, and baryon form factors and decay parameters.

With larger data samples at BESIII, more exciting physics results are hopefully to be obtained in the near future [101]. For the data taking plans in [101], BESIII has accumulated about 10 billion J/ψ events and 2.7 billion $\psi(3686)$ events. Currently, BESIII/BEPCII is running at 3.773 GeV to collect additional 17 fb^{-1} of $\psi(3770)$ data, which is hopefully to be finished in about two years. Then, BEPCII will optimize beam energy at 2.35 GeV and its peak luminosity is hopefully to be improved by 3-4 times compared to the current status. Moreover, BEPCII will also plan to extend the maximum energy up to 5.6 GeV. These will offer more effective data taking above 4.0 GeV and extend more physics opportunities.

References

[1] M. Ablikim *et al.* (BESIII Collaboration), Nucl. Instrum. Methods Phys. Res., Sect. A **614**, 345 (2010).

[2] D. M. Asner *et al.*, Int. J. Mod. Phys. A **24**, S1 (2009).

[3] M. Ablikim *et al.* (BESIII Collaboration), Phys. Rev. D **89**, 051104 (2014).

[4] M. Ablikim *et al.* (BESIII Collaboration), Phys. Rev. Lett. **123**, 211802 (2019).

[5] M. Ablikim *et al.* (BESIII Collaboration), Phys. Rev. Lett. **122**, 071802 (2019).

[6] M. Ablikim *et al.* (BESIII Collaboration), Phys. Rev. D **104**, 032001 (2021).

[7] M. Ablikim *et al.* (BESIII Collaboration), Phys. Rev. D **104**, 052009 (2021).

[8] M. Ablikim *et al.* (BESIII Collaboration), Phys. Rev. Lett. **127**, 171801 (2021).

[9] M. Ablikim *et al.* (BESIII Collaboration), Phys. Rev. D **92**, 072012 (2015).

[10] M. Ablikim *et al.* (BESIII Collaboration), Phys. Rev. D **96**, 012002 (2017).

[11] M. Ablikim *et al.* (BESIII Collaboration), Phys. Rev. D **92**, 112008 (2015).

[12] M. Ablikim *et al.* (BESIII Collaboration), Phys. Rev. Lett. **122**, 011804 (2019).

[13] M. Ablikim *et al.* (BESIII Collaboration), Phys. Rev. Lett. **122**, 121801 (2019).

[14] M. Ablikim *et al.* (BESIII Collaboration), Phys. Rev. D **97**, 092009 (2018).

[15] M. Ablikim *et al.* (BESIII Collaboration), Phys. Rev. Lett. **124**, 231801 (2020).

[16] M. Ablikim *et al.* (BESIII Collaboration), Phys. Rev. Lett. **122**, 061801 (2019).

[17] M. Ablikim *et al.* (BESIII Collaboration), Phys. Rev. Lett. **121**, 171803 (2018).

[18] M. Ablikim *et al.* (BESIII Collaboration), Phys. Rev. D **104**, L091103 (2021).

[19] M. Ablikim *et al.* (BESIII Collaboration), Eur. Phys. J. C **76**, 369 (2016).

[20] M. Ablikim *et al.* (BESIII Collaboration), Phys. Rev. D **101**, 072005 (2020).

[21] M. Ablikim *et al.* (BESIII Collaboration), Phys. Rev. D **97**, 012006 (2018).

[22] M. Ablikim *et al.* (BESIII Collaboration), Phys. Lett. B **767**, 42 (2017).

[23] M. Ablikim *et al.* (BESIII Collaboration), Phys. Rev. Lett. **121**, 081802 (2018).

[24] M. Ablikim *et al.* (BESIII Collaboration), Phys. Rev. Lett. **122**, 062001 (2019).

[25] M. Ablikim *et al.* (BESIII Collaboration), Phys. Rev. Lett. **123**, 231801 (2019).

[26] M. Ablikim *et al.* (BESIII Collaboration), Phys. Rev. Lett. **127**, 131801 (2021).

[27] M. Ablikim *et al.* (BESIII Collaboration), Phys. Rev. Lett. **124**, 241802 (2020); Phys. Rev. D **101**, 112002 (2020).

[28] M. Ablikim *et al.* (BESIII Collaboration), Phys. Rev. D **102**, 052008 (2020).

[29] M. Ablikim *et al.* (BESIII Collaboration), JHEP **05**, 164 (2021).

[30] M. Ablikim *et al.* (BESIII Collaboration), Phys. Rev. Lett. **115**, 221805 (2015).

[31] M. Ablikim *et al.* (BESIII Collaboration), Phys. Rev. Lett. **116**, 052001 (2016).

[32] M. Ablikim *et al.* (BESIII Collaboration), Phys. Rev. Lett. **118**, 112001 (2017).

[33] M. Ablikim *et al.* (BESIII Collaboration), Phys. Rev. Lett. **117**, 232002 (2016).

[34] M. Ablikim *et al.* (BESIII Collaboration), Phys. Rev. Lett. **121**, 062003 (2018).

[35] M. Ablikim *et al.* (BESIII Collaboration), Phys. Rev. Lett. **121**, 251801 (2018).

[36] J. Z. Bai *et al.* (BES Collaboration), Phys. Rev. Lett. **91**, 022001 (2003).

[37] M. Ablikim *et al.* (BESIII Collaboration), Phys. Rev. Lett. **108**, 112003 (2012).

[38] M. Ablikim *et al.* (BES Collaboration), Phys. Rev. Lett. **95**, 262001 (2005).

[39] M. Ablikim *et al.* (BESIII Collaboration), Phys. Rev. Lett. **106**, 072002 (2011).

[40] M. Ablikim *et al.* (BESIII Collaboration), Phys. Rev. Lett. **107**, 182001 (2011).

[41] M. Ablikim *et al.* (BESIII Collaboration), Phys. Rev. D **87**, 032008 (2013).

[42] M. Ablikim *et al.* (BESIII Collaboration), Phys. Rev. D **88**, 091502 (2013).

[43] M. Ablikim *et al.* (BESIII Collaboration), Phys. Rev. Lett. **115**, 091803 (2015).

[44] M. Ablikim *et al.* (BESIII Collaboration), Phys. Rev. Lett. **117**, 042002 (2016).

[45] M. Ablikim *et al.* (BESIII Collaboration), Phys. Rev. D **97**, 051101 (2018).

[46] M. Ablikim *et al.* (BESIII Collaboration), Eur. Phys. J. C **80**, 746 (2020).

[47] M. Ablikim *et al.* (BESIII Collaboration), Phys. Rev. D **103**, 012009 (2021).

[48] M. Ablikim *et al.* (BESIII Collaboration), Phys. Rev. Lett. **122**, 142002 (2019).

[49] M. Ablikim *et al.* (BESIII Collaboration), Phys. Rev. Lett. **127**, 121802 (2021).

[50] S. K. Choi *et al.* (Belle Collaboration), Phys. Rev. Lett. **91**, 262001 (2003).

[51] M. Ablikim *et al.* (BESIII Collaboration), Phys. Rev. Lett. **112**, 092001 (2014).

[52] M. Ablikim *et al.* (BESIII Collaboration), Phys. Rev. Lett. **122**, 202001 (2019).

[53] M. Ablikim *et al.* (BESIII Collaboration), Phys. Rev. Lett. **122**, 232002 (2019).

[54] M. Ablikim *et al.* (BESIII Collaboration), Phys. Rev. Lett. **124**, 242001 (2020).

[55] J. P. Lees *et al.* (BaBar Collaboration), Phys. Rev. D **86**, 051102 (2012).

[56] J. P. Lees *et al.* (BaBar Collaboration), Phys. Rev. D **89**, 111103 (2014).

[57] M. Ablikim *et al.* (BESIII Collaboration), Phys. Rev. Lett. **118**, 092001 (2017).

[58] M. Ablikim *et al.* (BESIII Collaboration), Phys. Rev. Lett. **118**, 092002 (2017).

[59] M. Ablikim *et al.* (BESIII Collaboration), Phys. Rev. Lett. **122**, 102002 (2019).

[60] M. Ablikim *et al.* (BESIII Collaboration), Phys. Rev. D **99**, 091103 (2019).

[61] M. Ablikim *et al.* (BESIII Collaboration), Phys. Rev. D **102**, 031101 (2020).
[62] M. Ablikim *et al.* (BESIII Collaboration), Phys. Rev. D **102**, 012009 (2020).
[63] M. Ablikim *et al.* (BESIII Collaboration), Phys. Rev. D **104**, 052012 (2021).
[64] M. Ablikim *et al.* (BESIII Collaboration), Phys. Rev. D **102**, 112009 (2020).
[65] M. Ablikim *et al.* (BESIII Collaboration), Phys. Rev. D **101**, 012008 (2020).
[66] M. Ablikim *et al.* (BESIII Collaboration), Phys. Rev. D **103**, 032006 (2021).
[67] M. Ablikim *et al.* (BESIII Collaboration), Phys. Rev. Lett. **110**, 252001 (2013).
[68] M. Ablikim *et al.* (BESIII Collaboration), Phys. Rev. Lett. **115**, 112003 (2015).
[69] M. Ablikim *et al.* (BESIII Collaboration), Phys. Rev. Lett. **112**, 022001 (2014).
[70] M. Ablikim *et al.* (BESIII Collaboration), Phys. Rev. Lett. **115**, 222002 (2015).
[71] M. Ablikim *et al.* (BESIII Collaboration), Phys. Rev. D **92**, 092006 (2015).
[72] M. Ablikim *et al.* (BESIII Collaboration), Phys. Rev. Lett. **111**, 242001 (2013).
[73] M. Ablikim *et al.* (BESIII Collaboration), Phys. Rev. Lett. **113**, 212002 (2014).
[74] M. Ablikim *et al.* (BESIII Collaboration), Phys. Rev. Lett. **112**, 132001 (2014).
[75] M. Ablikim *et al.* (BESIII Collaboration), Phys. Rev. Lett. **115**, 182002 (2015).
[76] M. Ablikim *et al.* (BESIII Collaboration), Phys. Rev. Lett. **126**, 102001 (2021).
[77] R. Aaij *et al.* (LHCb Collaboration), Phys. Rev. Lett. **127**, 082001 (2021).
[78] M. Ablikim *et al.* (BES Collaboration), Phys. Rev. Lett. **101**, 102004 (2008).
[79] M. Ablikim *et al.* (BESIII Collaboration), Phys. Rev. Lett. **127**, 082002 (2021).
[80] M. Ablikim *et al.* (BESIII Collaboration), Phys. Rev. D **104**, L091104 (2021).
[81] M. Ablikim *et al.* (BESIII Collaboration), Phys. Rev. D **104**, 112009 (2021).
[82] B. Aubert *et al.* (BaBar Collaboration), Phys. Rev. D **74**, 091103 (2006).
[83] C. P. Shen *et al.* (Belle Collaboration), Phys. Rev. D **80**, 031101 (2009).
[84] M. Ablikim *et al.* (BES Collaboration), Phys. Rev. Lett. **100**, 102003 (2008).
[85] M. Ablikim *et al.* (BESIII Collaboration), Phys. Rev. D **100**, 032009 (2019).
[86] M. Ablikim *et al.* (BESIII Collaboration), Phys. Rev. D **99**, 032001 (2019).
[87] M. Ablikim *et al.* (BESIII Collaboration), Phys. Rev. Lett. **124**, 112001 (2020).
[88] M. Ablikim *et al.* (BESIII Collaboration), Phys. Rev. D **102**, 012008 (2020).
[89] M. Ablikim *et al.* (BESIII Collaboration), Phys. Rev. D **104**, 032007 (2021).
[90] M. Ablikim *et al.* (BESIII Collaboration), Phys. Rev. D **104**, 092014 (2021).
[91] M. Ablikim *et al.* (BESIII Collaboration), Phys. Lett. B **813**, 136059 (2021).
[92] M. Ablikim *et al.* (BESIII Collaboration), Phys. Rev. D **99**,112008 (2019).
[93] M. Ablikim *et al.* (BESIII Collaboration), Phys. Rev. D **91**, 112004 (2015).
[94] M. Ablikim *et al.* (BESIII Collaboration), Phys. Rev. Lett. **124**, 042001 (2020).
[95] M. Ablikim *et al.* (BESIII Collaboration), Phys. Rev. D **99**, 092002 (2019).
[96] M. Ablikim *et al.* (BESIII Collaboration), Phys. Lett. B **817**, 136328 (2021).
[97] M. Ablikim *et al.* (BESIII Collaboration), Nature Phys. **17**, 1200 (2021).
[98] M. Ablikim *et al.* (BESIII Collaboration), Phys. Rev. Lett. **123**, 122003 (2019).
[99] M. Ablikim *et al.* (BESIII Collaboration), Nature Phys. **15**, 631 (2019).
[100] M. Ablikim *et al.* (BESIII Collaboration), Phys. Rev. Lett. **125**, 052004 (2020).
[101] M. Ablikim *et al.* (BESIII Collaboration), Chin. Phys. C **44**, 040001 (2020).